Jia *et al. Respiratory Research* (2025) 26:103
https://doi.org/10.1186/s12931-025-03189-7

Respiratory Research

RESEARCH Open Access

Immunological landscape of children with *Mycoplasma pneumoniae* pneumonia in the post-COVID-19 era reveals distinctive severity indicators

Ran Jia[1†], Haiyan Guo[2,3,4†], Aizhen Lu[5†], Caiyan Zhang[2], Yuanyuan Qi[5], Dingmei Wang[5], Wen He[5], Qing Wang[5], Zimei Cheng[2], Yajing Gao[2,3,4], Guoping Lu[2], Libo Wang[5], Xiaowen Zhai[6], Jin Xu[1,7*†], Xiaobo Zhang[5*†], Yi Wang[8*†] and Yufeng Zhou[2,3,4,9*†]

Abstract

Background There is a recent global surge in *Mycoplasma pneumoniae* pneumonia (MPP). However, the key immune factors that contribute to the advancement of the disease remain unknown. Hence, we conducted this study to uncover the immunological profile in children affected by MPP.

Methods This study enrolled children visiting Children's Hospital of Fudan University from December 2023 to April 2024, including 34 healthy controls, 51 severe MPP (S-MPP), 27 non-severe MPP (NS-MPP), and 34 non-MPP pneumonia (NMP) cases. Their blood samples were analyzed using flow cytometry, multi-cytokine assays, and antibody detection methods.

Results Compared with NMP cases, MPP cases displayed higher frequencies of natural killer T cells, classical monocytes, and monocytic myeloid-derived suppressor cells. Notably, both T helper type 1 and activated regulatory T cells were more abundant in MPP cases, particularly in S-MPP, whereas CD8 + T cells displayed an exhaustion phenotype. The proportion of naïve B cells was reduced, while functional B cells, including memory B cells and plasmablasts, increased in S-MPP. 12 out of 95 clinical laboratory indicators and 3 out of 48 cytokines significantly

†Ran Jia, Haiyan Guo and Aizhen Lu contributed equally to this work as co-first authors.

†Jin Xu, Xiaobo Zhang, Yi Wang and Yufeng Zhou contributed equally to this work as co-senior authors.

*Correspondence:
Jin Xu
jinxu_125@163.com
Xiaobo Zhang
zhangxiaobo0307@163.com
Yi Wang
yiwang@shmu.edu.cn
Yufeng Zhou
yfzhou1@fudan.edu.cn

Full list of author information is available at the end of the article

Background

Mycoplasma pneumoniae (MP) is responsible for 40% of community-acquired pneumonia (CAP) cases in children, particularly in school-aged children and adolescents [1]. MP infections are usually endemic, and epidemics occur every 1–7 years [1, 2]. As reported, the closest MP epidemic was reported in late 2019–early 2020 across various regions worldwide, primarily in Europe and Asia [2], with the exception of China. This global epidemic was controlled by non-pharmaceutical interventions implemented to manage coronavirus disease 2019 (COVID-19). However, during 2023–2024, an

differed between S-MPP and NS-MPP. Finally, we performed logistic and LASSO regression analyses and developed a predictive model for S-MPP that incorporates naïve B cell percentage from flow cytometry, cholinesterase from clinical laboratory tests, and interleukin 18 from the cytokine assay.

Conclusions These results clarify the immunological features in pediatric MPP cases, and identify novel markers for severe cases, providing insights for early diagnosis and immunological management in affected children.

Keywords *Mycoplasma pneumonia* pneumonia, Children, Immunological landscape, Severity indicator

MP outbreak among children, particularly those under 15, has been reported in multiple regions [3, 4], including China [5, 6]. As proposed by Li et al. [7], the current MP outbreak may represent a "delayed" resurgence after the conclusion of China's "Zero-COVID" policy.

MP pneumonia (MPP) is usually a benign, self-limiting disease that generally responds well to macrolide antibiotics [7]. However, the currently prevalent MP strains are largely macrolide-resistant, leading to a more complex and potentially life-threatening condition known as refractory MPP (RMPP) [8]. Regarding the disease progression, there is evidence that excessive host immune responses are closely associated with severity, such as elevated serum levels of inflammatory cytokines [9]. This evidence is supported by observations that MP infection-mediated lung injury is greatly reduced in immunodeficient hosts [10]. Thus, early corticosteroid therapy with antibiotics is routinely utilized in MPP treatment. Although studies thus far have provided important insights into MPP progression, the specific immune cells contributing to immune dysregulation in MPP remain unexplored. Accordingly, there is a need for comprehensive immune profiling of children with MPP, especially in severe cases. Hence, this study was conducted to characterize the immune response landscape in children with MPP. We performed flow cytometry, multiple cytokine analysis, and antibody detection to reveal distinct immune response patterns in children with MPP and to identify novel markers for severe cases, offering valuable guidance for early diagnosis and immunological management in affected children.

Methods

Patients and samples

This study enrolled 112 pneumonia cases and 34 healthy controls (HCs), which visited or were hospitalized at the Children's Hospital of Fudan University from December 2023 to April 2024. The pneumonia cases included 34 non-MP pneumonia (NMP) cases and 78 MPP cases, including 51 severe MPP (S-MPP) and 27 non-severe MPP (NS-MPP). MPP cases were categorized based on the *Guidelines for Diagnosis and Treatment of Community-Acquired Pneumonia in Children* (2019 version) (Additional file) [11]. All blood samples were collected from patients on the first day of hospitalization.

Flow cytometry analysis

Whole blood cells were placed into sterilized tubes and blocked with Fc block for 20 min at 4 °C, then stained with fluorescent antibodies for 30 min at 4 °C. The antibodies were listed in Additional file. Red blood cells were lysed using BD FACS Lysing Solution 10x Concentrate (BD#349202) for 10 min at room temperature. The cells were subsequently analyzed using a BD FACSCanto II Flow Cytometer, and the data were processed with FlowJo software (version 10.9.0). All blood samples were subjected to flow cytometry assay on the day of collection, and all the experiments were conducted under consistent conditions (including the same operator and analyzer) to minimize the batch difference.

Cytokine assay

We measured the plasma concentrations of 48 cytokines, including β-NGF, CTACK/CCL27, Eotaxin/CCL11, FGF-basic, G-CSF, GM-CSF, GRO-α (Gro-α/KC/CXCL1), HGF, IFN-α2, IFN-γ, IL-1α, IL-1Rα, IL-2Rα, IL-1β, IL-2, IL-3, IL-4, IL-5, IL-6, IL-7, IL-8/CXCL8, IL-9, IL-10, IL-12(p40), IL-12(p70), IL-13, IL-15, IL-16, IL-17 A, IL-18, IP-10/CXCL10, LIF, M-CSF, MCP-1/CCL2, MCP-3/CCL7, MIG, MIP-1α/CCL3, MIP-1β, MIF, PDGF-BB, RANTES, SCF, SCGF-β, SDF-1α, TRAIL, TNF-α, TNF-β, and VEGF-A in human samples using a Luminex multiplex cytokine kit (Cat. LXLBH48-1), in accordance with the manufacturer's instructions. To be noted, of the 48 cytokines tested, 10 (IL-2, IL-6, IL-5, IL-15, IL-12p70, GM-CSF, Basic FGF, VEGF, β-NGF, and GRO-α) were below the detection limit in most samples, thus excluded from further analysis.

Anti-MP and anti-SARS-CoV-2 IgG and IgM detection

We quantified antibodies targeting MP and SARS-CoV-2 using a clinical-grade chemiluminescence immunoassay kit (YHLO Biotech, China), which included an anti-SARS-CoV-2 IgM kit (YHLO#C86095M), an anti-SARS-CoV-2 IgG kit (YHLO#C86095G), an anti-MP IgM kit (YHLO#C88004M), and an anti-MP IgG kit (YHLO#C88003G). Samples were processed using the iFlash 3,000 chemiluminescence immunoassay analyzer (YHLO Biotech, China).

Statistical analysis

Continuous data were presented as medians with interquartile ranges (IQRs); categorical data were expressed as medians with percentages. The chi-square test or Fisher's exact test was used to compare the proportions of categorical variables. In the analysis of continuous data for two-group comparisons, normally distributed variables with equal variances were analyzed using the unpaired Student's *t*-test, while the Welch-adjusted *t*-test was applied to accommodate unequal variances. Non-normally distributed variables were assessed via the Mann-Whitney *U* test. In multi-group comparisons (≥ 3 groups), one-way ANOVA with Bonferroni post-hoc testing was used for normally distributed data under equal variance assumptions. For normally distributed data with unequal variances, Welch ANOVA followed by Dunnett T3 post-hoc analysis was employed. Non-normally distributed multi-group data were evaluated using the Kruskal-Wallis test, with Dunn's test for post-hoc pairwise comparisons. These statistical analyses were performed using GraphPad Prism software (version 10) and IBM SPSS Statistics software (version 23). Two-sided *p*-values of < 0.05 were considered statistically significant.

Univariate logistic analysis was performed to identify independent risk factors for S-MPP and to explore potential risk factors associated with the condition. Subsequently, least absolute shrinkage and selection operator (LASSO) regression was applied to reduce data dimensionality. LASSO regression achieves this reduction by applying a penalty function that shrinks the coefficients of non-significant variables to zero, facilitating the selection of relevant feature variables. Finally, multifactor logistic regression analysis was performed to investigate risk factors for S-MPP. The predictive model was developed using DecisionLinnc 1.0.

Results

Prevalence of MP infections among children in the post-COVID-19 era

We found that both the MP detection rate and number of MP-positive cases significantly increased in the post-COVID-19 era. The peak detection rate (55.4%) and highest number of positive cases (767 cases) occurred in October 2023, representing the largest recorded values in the past 6 years (Supplementary Fig. 1). These results indicated that children in Shanghai experienced an unusual MP outbreak after the end of the "Zero-COVID" policy.

Demographic and clinical characteristics of children with MPP

A total of 112 pneumonia cases with available clinical data were included in our study, comprising 51 cases of S-MPP, 27 cases of NS-MPP, and 34 cases of NMP. The flowchart of the enrollment process and the subsequent data collection were illustrated (Fig. 1A, B). Due to limitations in the availability of both tests, not all samples could be included in the multiple cytokine and antibody assays. Notably, there were no significant differences among the four groups in terms of age or sex within any of the three cohorts (Fig. 1C).

Next, we summarized the clinical characteristics of the MPP cases (Supplementary Table 1). In total, 77 patients (98.72%) presented with fever; 54 (69.23%) experienced high fever (≥ 39 °C) and 20 (25.64%) exhibited extremely high fever (≥ 40 °C). The median (IQR) duration of fever was 7.5 [5, 6, 7, 8, 9, 10] days. Regarding treatment, 77 patients (98.72%) received glucocorticoids, seven patients (8.97%) were administered anticoagulants, and two S-MPP patients were given intravenous immunoglobulin (IVIG). Antibiotic monotherapy was used in only eight MPP cases (10.26%), whereas combination antibiotic therapy was administered in the remaining 70 cases (89.74%). Quinolone antibiotics were widely used in children with MPP, particularly in severe cases, with a utilization rate of 25 (49.02%). Complications were significantly more common in S-MPP patients than in NS-MPP patients. Pulmonary consolidation was the most frequent complication, observed in 58 patients (74.36%); its incidence was 84.31% in S-MPP cases. Collectively, S-MPP cases exhibited more pronounced clinical symptoms, a higher rate of complications, and required more complex therapeutic management, consistent with the severity classification.

Regarding clinical laboratory test results, 12 of 95 indicators significantly differed between the NS-MPP and S-MPP groups: total IgM, D-dimer, fibrinogen degradation products (FDP), lactate dehydrogenase (LDH), α-hydroxybutyrate dehydrogenase (α-HBDH), alkaline phosphatase (ALP), alanine aminotransferase (ALT), albumin (Alb), cholinesterase (ChE), partial pressure of carbon dioxide (PaCO2), pH, and hydrogen ion concentration (CH+) (Fig. 2A, B). The full names of the 95 indicators are provided in Supplementary Table 2. Notably, five indicators (ALP, Alb, ChE, $PaCO_2$, and CH+) were significantly lower in the S-MPP group than in the NS-MPP group (Fig. 2B). Among respiratory pathogens, adenovirus was the most common co-infecting pathogen with MP in both the NS-MPP (18.5%) and S-MPP (35.3%) groups; its prevalence was significantly higher in the latter group (Fig. 2C). In contrast, influenza B virus and influenza A virus were the two most prevalent pathogens in the NMP group (44.1% and 32.4%, respectively). Overall, compared with non-severe cases, S-MPP cases showed distinct clinical indicators upon hospitalization, including 12 blood parameters and co-infections, particularly with adenovirus.

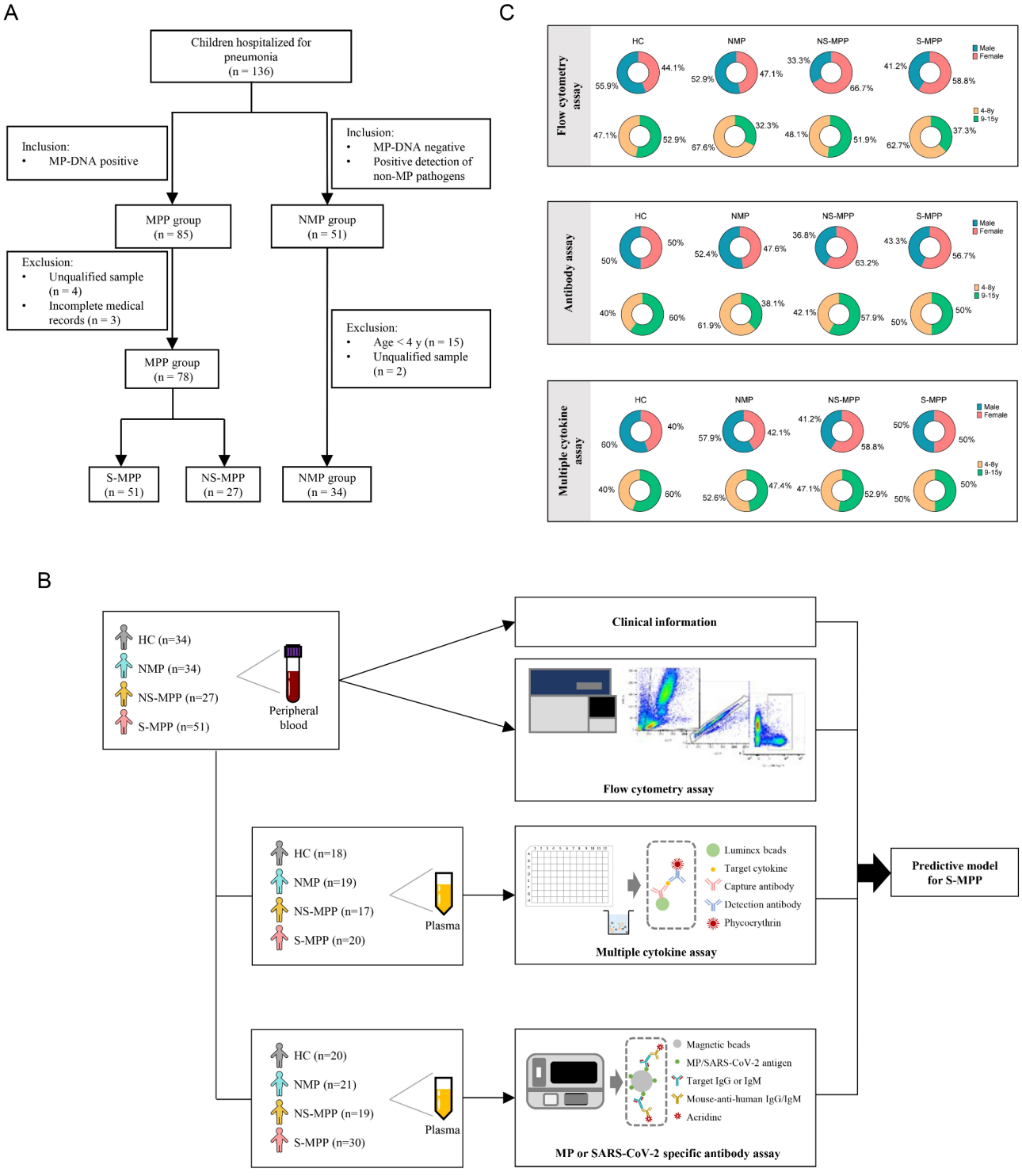

Fig. 1 Schematic overview of the study. **A**, Flowchart of the enrollment process. **B**, Description of the three cohorts subjected to different analyses. **C**, Age and sex distribution across the three cohorts. MPP, Mycoplasma pneumoniae pneumonia; NMP, pneumonia caused by non-MP pathogens; HC, healthy control; NS-MPP, non-severe MPP; S-MPP, severe MPP

Distinct immunological phenotypes in children with MPP

Flow cytometry analysis was conducted to examine 34 immune cell subsets (Figs. 3 and 4). The gating strategy is shown in Supplementary Fig. 2. Although all samples were collected upon hospitalization, the progression of the disease varied; MPP cases typically required hospitalization after >1 week of ineffective antibiotic treatment, whereas NMP cases were predominantly admitted at the

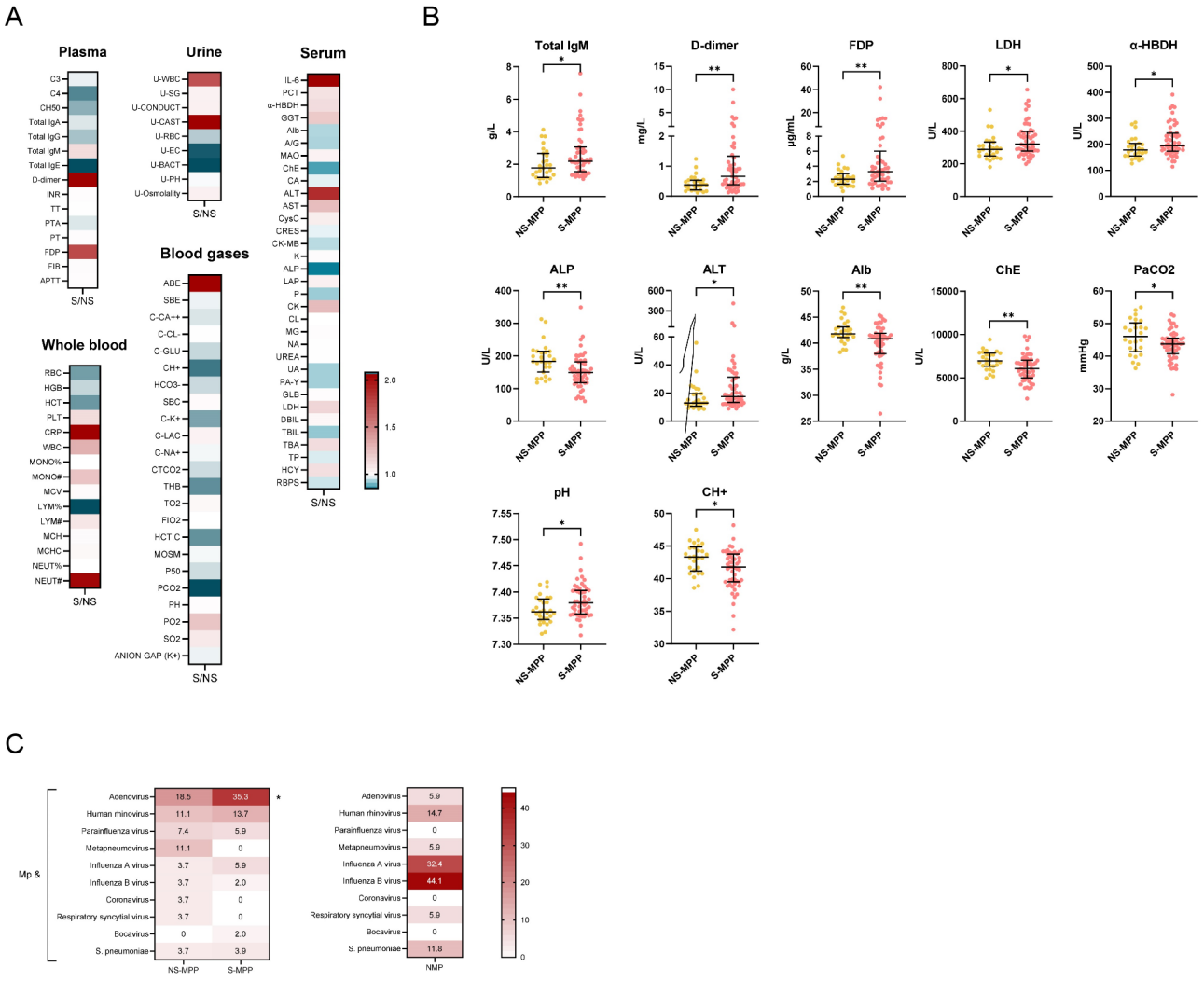

Fig. 2 Clinical laboratory indicators differing between children with NS-MPP and those with S-MPP. **A**, S-MPP/NS-MPP ratios across 95 available clinical laboratory indicators (abbreviations are provided in Supplementary Table 1). **B**, The 12 clinical laboratory indicators that are significantly different between the S-MPP and NS-MPP groups. **C**, Distributions of different pathogens. Data are presented as median ± IQR. *$p < 0.05$, **$p < 0.01$

onset of the disease. Thus, NMP group served as early-stage immunological controls for comparisons with MPP group.

Accordingly, consistent with the more advanced disease stage in the MPP group, some immune cells displayed a less pronounced response relative to the NMP group, as indicated by lower frequencies of myeloid DC (mDC), plasmacytoid DC (pDC) (Fig. 3A). Moreover, although the MPP group showed decreased proportion of mature natural killer (mNK) cells (Fig. 3B), they had a significantly higher frequency of natural killer T cells (NKT) than the other two groups (Fig. 3C). Notably, the MPP group displayed elevated classical monocytes (C-Mono) but reduced intermediate monocytes (INT-Mono) frequencies (Fig. 3D). Although the overall frequency of myeloid-derived suppressor cells (MDSC), known for their immunosuppressive effect on CD8 + T cells, was similar across all three groups, the MPP group displayed increased proportions of monocytic MDSC (M-MDSC) and early-stage MDSC (eMDSC), but a decreased proportion of polymorphonuclear MDSC (PMN-MDSC) compared with the NMP group (Fig. 3E). Additionally, no significant differences were observed between the S-MPP and NS-MPP groups for these innate immune cell types (Supplementary Fig. 3). In summary, MPP cases showed distinct characteristics in innate immune cells compared with the NMP group, particularly concerning higher frequencies of NKT, C-Mono, and M-MDSC.

Regarding T cells, whereas the proportions of total CD4 + T cells, naïve T (NT), effector memory T cells (TEM), CD45RA + effector memory T cells (TEMRA), and regulatory T cells (Treg) did not differ between the MPP and NMP groups (Supplementary Fig. 4A), the MPP group displayed a significantly higher frequency of

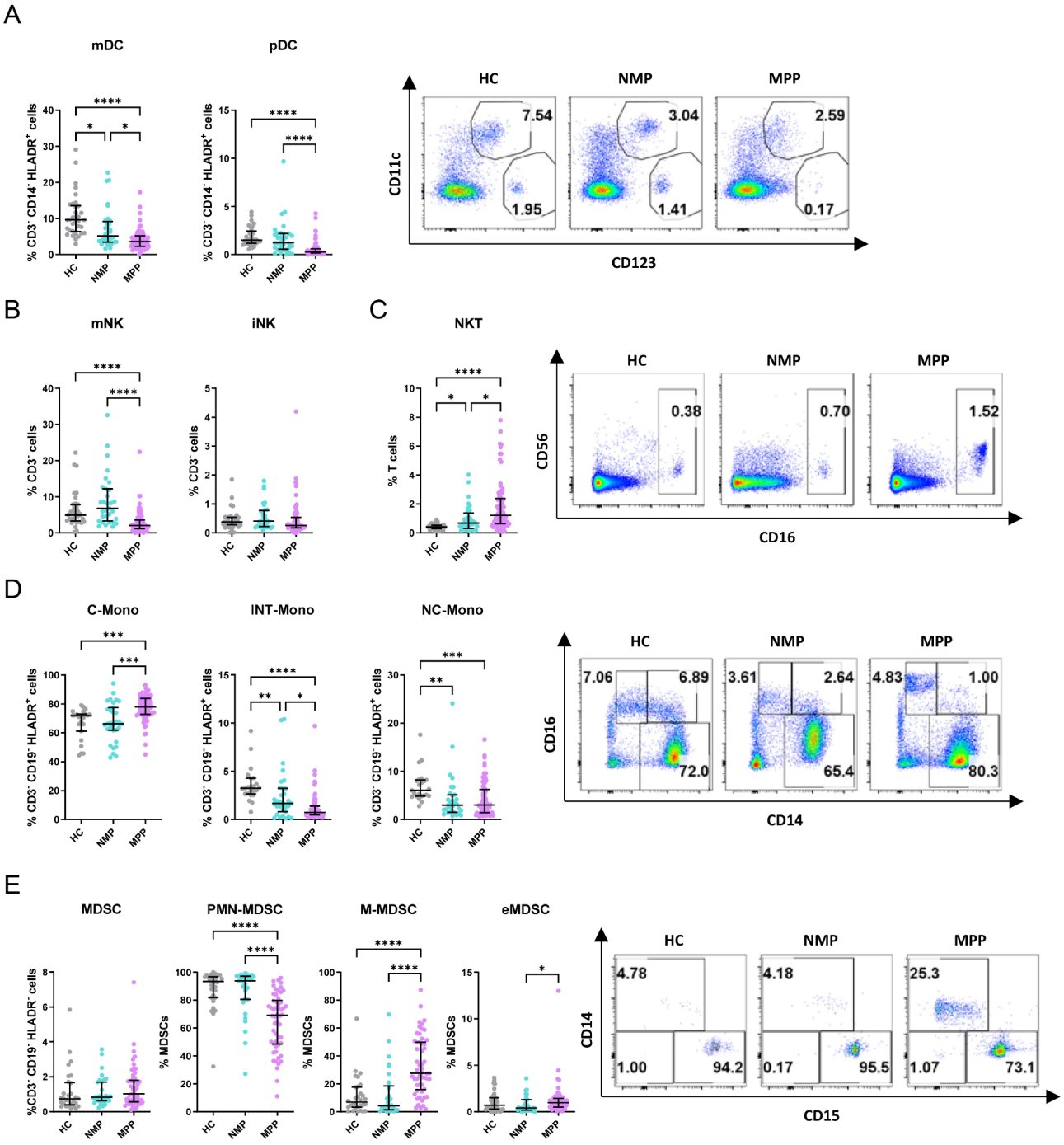

Fig. 3 Innate immune cell phenotypes in children with MPP. Proportions of various innate immune cells in PBMCs revealed by flow cytometry. **A**, DCs. **B**, NK cells. **C**, NKT cells. **D**, monocytes. **E**, MDSCs. Data are presented as median ± IQR. *$p < 0.05$, **$p < 0.01$, ***$p < 0.001$, and ****$p < 0.0001$. mDC, myeloid dendritic cell; pDC, plasmacytoid dendritic cell; mNK, mature NK cell; iNK, immature NK cell; NKT, natural killer T cell; C-Mono, classical monocyte; INT-Mono, intermediate monocyte; NC-Mono, non-classical monocyte; eMDSC, early-stage myeloid-derived suppressor cell; M-MDSC, monocytic MDSC; PMN-MDSC, polymorphonuclear MDSC

Th1 cells and activated Treg (Act Treg) than the NMP group; this trend was particularly pronounced in the S-MPP group (Fig. 4A, B). Notably, in the S-MPP group, the Th1 response appears to override the suppressive effect of Treg, as indicated by the elevated Th1/Treg ratio (Fig. 4C). Intriguingly, there was a modest increase in follicular helper T cells (Tfh) within the MPP group compared to the HC group (Fig. 4D). In contrast, follicular regulatory T cells (Tfr) exhibited a significantly higher proportion in the MPP group, with the S-MPP group

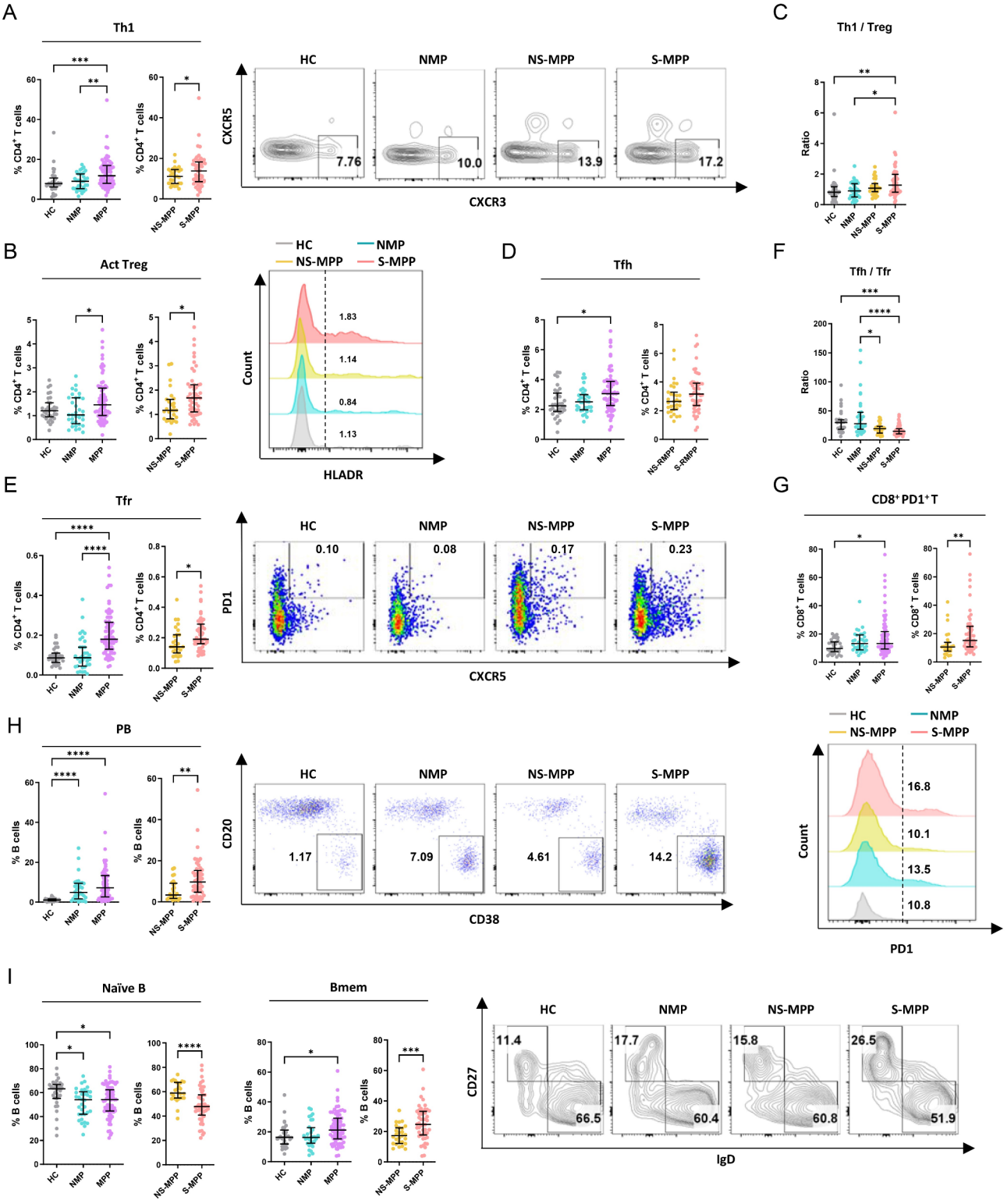

Fig. 4 Adaptive immune cell phenotypes in children with MPP. Frequencies of adaptive immune cells in PBMCs revealed by flow cytometry. **A**, Th1. **B**, Act Treg. **C**, Ratio of Th1/Treg. **D**, Tfh. **E**, Tfr. **F**, Ratio of Tfh/Tfr. **G**, CD8 + PD1 +T cells. **H**, PB. **I**, Naïve B and Bmem. Data are presented as median ± IQR. *$p < 0.05$, **$p < 0.01$, ***$p < 0.001$, and ****$p < 0.0001$. Th1, type 1 helper T cell; Treg, regulatory T cell; Tfr, T follicular regulatory cell; PB, plasmablast; Bmem, memory B cell

demonstrating a greater percentage than the NS-MPP group (Fig. 4E). Furthermore, the Tfh/Tfr ratio was lower in both the S-MPP and NS-MPP groups in comparison to the NMP group (Fig. 4F). Regarding CD8 + T cells, the MPP group showed an increased NT and decreased TEMRA cells (Supplementary Fig. 4B). Importantly, S-MPP group showed a higher PD1 expression (Fig. 4G). Taken together, these findings suggested an enhanced Th1 response and exhausted CD8 + T cell response in the MPP group; both trends were more pronounced in S-MPP cases.

With respect to B cell subsets, the MPP group showed a reduced percentage of naïve B cells relative to the HC group; however, it had increased percentages of functional B cells, such as memory B cells (Bmem) and plasmablasts (PB) (Fig. 4H, I; Supplementary Fig. 4C). These changes were particularly prominent in the S-MPP group relative to the NS-MPP group, suggesting considerable stimulation of the B cell response in MPP cases, especially those involving S-MPP patients.

Cytokine and antibody profiles in MPP patients

Among the 48 cytokines tested, 34 were significantly elevated in the NMP group compared with the MPP group (Fig. 5A; Supplementary Fig. 5), possibly due to the later disease stage and early glucocorticoid treatment in MPP cases. Notably, three cytokines—monokine induced by interferon-γ (MIG), interleukin-18 (IL-18), and interleukin-2 receptor subunit α (IL-2Rα)—exhibited significantly higher levels in the S-MPP group than in the

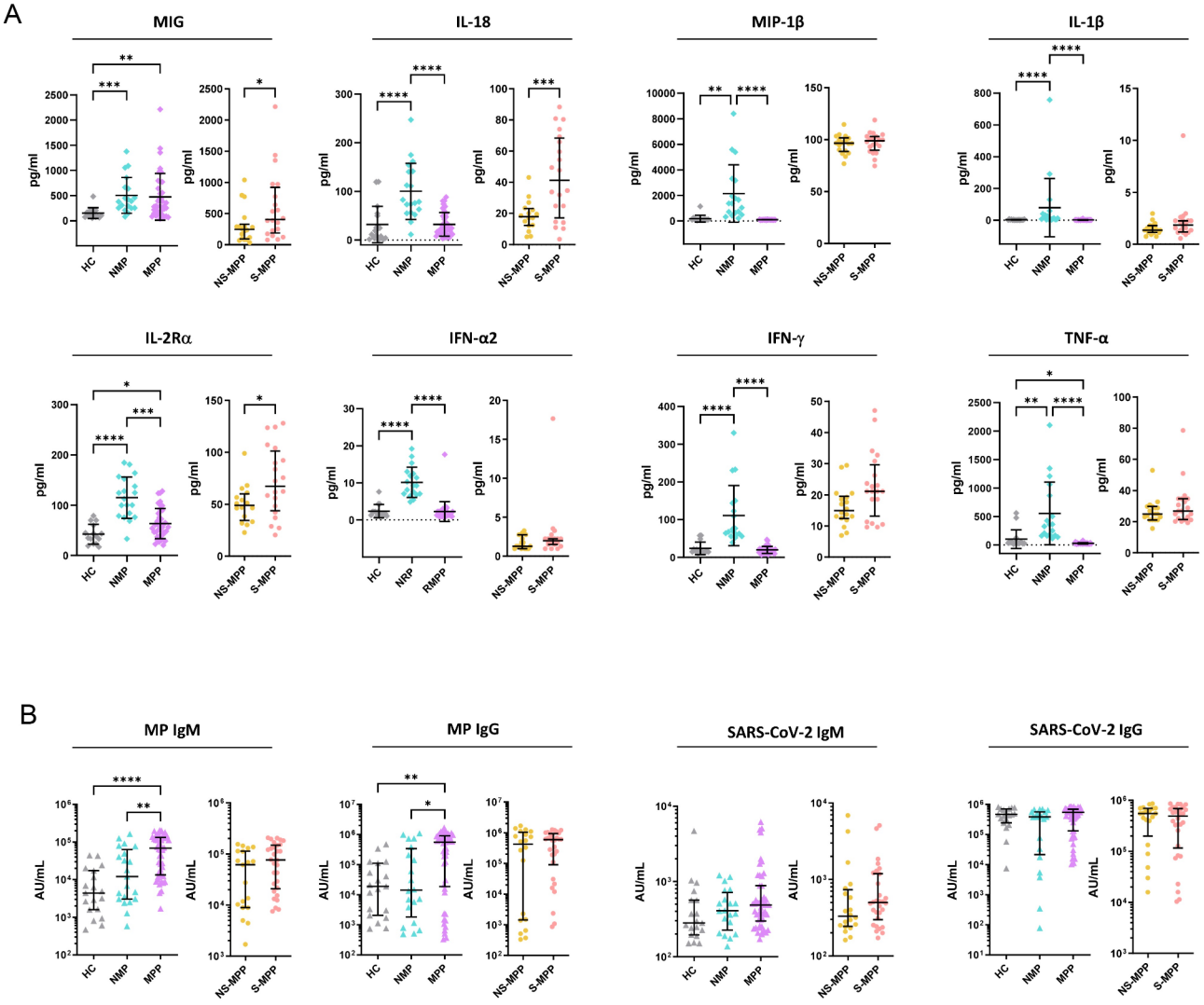

Fig. 5 Levels of various cytokines and MP/SARS-CoV-2-specific antibodies in children with MPP. **A**, Cytokine concentrations in different groups. **B**, Levels of MP/SARS-CoV-2-specific IgM and IgG in different groups. Data are presented as median ± IQR. *$p < 0.05$, **$p < 0.01$, ***$p < 0.001$, and ****$p < 0.0001$. MIG, monokine induced by interferon-γ; IL-18, interleukin 18; MIP-1β, macrophage inflammatory protein-1β; IL-2Rα, interleukin 2 receptor subunit α; IFN, interferon; TNF, tumor necrosis factor

NS-MPP group (Fig. 5A). Concerning antibody levels, as expected, both MP-specific IgM and IgG were elevated in the MPP group relative to the other groups (Fig. 5B). Additionally, no significant differences were observed in SARS-CoV-2-specific IgM and IgG levels among our patients (Fig. 5B). These findings indicate that, despite glucocorticoid treatment, S-MPP cases exhibited a distinct cytokine response pattern relative to NS-MPP cases, characterized by substantially higher levels of MIG, IL-18, and IL-2Rα.

Development of a predictive model for SMPP

Based on the features of S-MPP cases identified using clinical information, flow cytometry analysis, and cytokine tests, we initially selected 36 potential risk factors associated with S-MPP by univariate logistic analysis. Further, we selected 25 variables with p-values < 0.05 for LASSO dimensionality reduction (Supplementary Fig. 6; Supplementary Table 3). ChE (from clinical laboratory tests), naïve B cell percentage (from flow cytometry), and IL-18 (from cytokine assay)—were identified as predictive factors (Supplementary Table 4). Multivariable logistic regression analysis indicated that IL-18 is a risk factor for S-MPP, whereas ChE and naïve B cell percentage serve as protective factors (Supplementary Table 4). The regression equation is as follows: logit(p) = 6.68 − (0.001 * ChE) − (0.066 * naïve B cell percentage) + (0.034 * IL-18).

A calibration curve was built to assess the logistic regression model's performance (Fig. 6A). A logistic regression coefficient plot displayed the coefficients' magnitude and direction for the predictive variables (Fig. 6B). The model exhibited good fit and residual patterns, as shown in the residual plot (Fig. 6C). A DCA plot illustrated the model's clinical utility for S-MPP prediction (Fig. 6D). Forest plots and receiver operating characteristic curves were generated (Fig. 6E, F), with an AUC of 0.844, indicating that the model has a strong discriminatory ability in distinguishing between NS-MPP and S-MPP. To estimate the risk of S-MPP, ChE, naïve B cell percentage, and IL-18 were incorporated into a nomogram based on multivariate analysis results (Fig. 6G). Supplementary Fig. 7 displays the predictive model graph after multiple imputations for the variable IL-18. Overall, we successfully developed a novel predictive model incorporating ChE, naïve B cell percentage, and IL-18 to identify S-MPP cases upon hospitalization.

Discussion

In this study, we performed a comprehensive analysis to elucidate the immunological and clinical characteristics of children with MPP, particularly S-MPP, which may aid efforts to develop immunological strategies for MPP treatment. Additionally, we developed a new predictive model for S-MPP that could serve as a valuable reference in the clinical assessment of MPP cases.

Th1 cells, mainly producing IL-2 and IFN-γ, are well-established to help control infections involving intracellular pathogens. However, Th1 responses can also drive inflammation in various diseases, including autoimmune disorders (e.g., multiple sclerosis, rheumatoid arthritis) [12] and infectious diseases (e.g., influenza, COVID-19, MPP) [13]. The positive association between Th1 response and MPP severity has been confirmed in both previous studies [9] and our findings. Based on our findings and those of other researchers, we propose several possible explanations. First, Wang et al.. reported that the community-acquired respiratory distress syndrome (CARDS) toxin of MP promotes Th1 differentiation in a dose- and time-dependent manner [14]. Second, the elevated IL-18 in S-MPP cases might also enhance the Th1 response, since IL-18 receptor (IL-18R)-deficient mice have been proved to show an impaired Th1 response [15] but lower levels of lung injury [16]. Third, Paul et al. demonstrated that α-galactosylceramide (α-GalCer)-driven activation of natural killer T (NKT) cells, predominantly the invariant NKT (iNKT) subset, suppresses melanoma tumor progression through enhanced Th1 recruitment [17]. Hence, the higher NKT frequencies in MPP cases might also contribute to the elevated Th1. Further investigation is needed to validate the above hypothesis.

Treg cells suppress both adaptive and innate immunity, particularly by limiting excessive activation of effector T cells and the maturation of antigen-presenting cells (APCs). In severe infections, such as sepsis, increased Treg levels have been linked to worse prognosis [18]. Consistent with our findings, Takahashi et al. reported that MP infection could induce impaired and persistent Treg responses [19], which may explain why MP infection is associated with allergic and autoimmune diseases [20]. Intriguingly, Koch et al. suggested that an excessive Th1 response can lead to partial and incomplete Th1 differentiation, thereby inducing functionally specialized Treg cells to counter the pro-inflammatory effects of Th1 activity [21]. Thus, the increased frequency of activated Treg, also known as effector Treg (eTreg) [22], in S-MPP may partly result from potentially excessive but defective Th1 differentiation, although further validation is needed.

Upon activation, some activated B cells migrate to the extrafollicular region, where they differentiate into numerous short-lived plasmablasts and secrete substantial quantities of antibodies [23, 24]. Subsequently, other activated B cells enter the follicle, initiating a germinal center reaction, resulting in the production of Bmem and a limited number of long-lived plasmablasts [23, 24]. Hence, the elevated frequencies of Bmem and plasmablasts observed in S-MPP cases indicate a robust response in both the extrafollicular and germinal

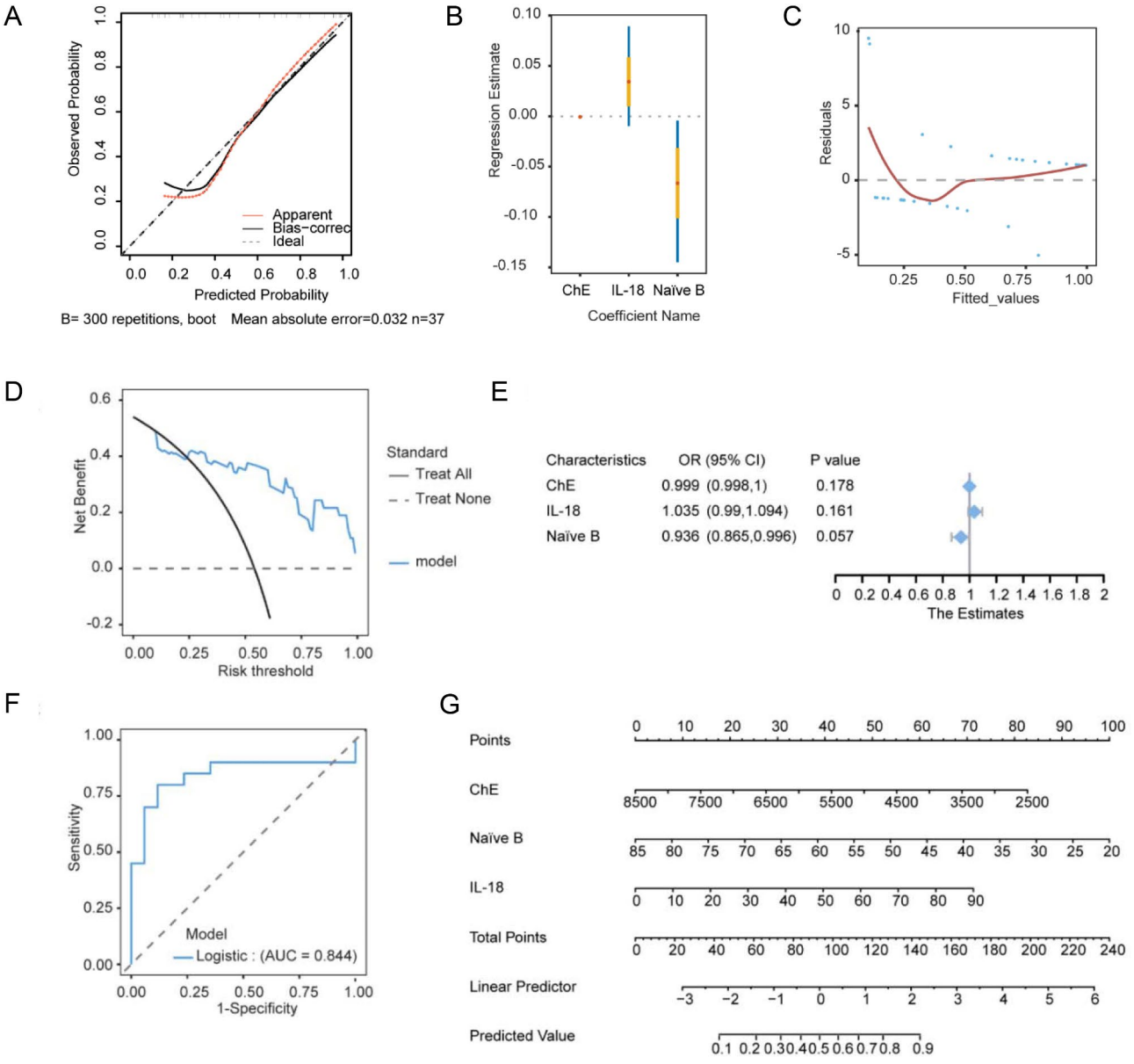

Fig. 6 Establishment and clinical application of predictive model for S-MPP. **A**, Logistic regression calibration curve. **B**, Logistic regression coefficient plot. **C**, Logistic regression fitted values and residuals plot. **D**, Decision curve analysis (DCA) plot. **E**, Logistic regression forest plot. **F**, Logistic regression receiver operating characteristic curve plot. **G**, Nomogram for predicting S-MPP. ChE, cholinesterase; IL-18, interleukin 18

center pathways. However, it is remarkable that the S-MPP group displayed a higher frequency of plasmablasts cells without a corresponding increase in MP-specific antibodies relative to NS-MPP cases, suggesting a potential deficiency in antibody production by plasmablasts cells in severe cases. A plausible explanation for this phenomenon could be the significant increase in Tfr cells observed in S-MPP cases, which are recognized for their role in dynamically suppressing the antibody production of B cells [25, 26]. This hypothesis warrants additional investigation.

Our data revealed elevated NKT cell percentages in MPP patients, in contrast to a decrease in mNK cells. This pattern aligns with observations made in murine models of breast cancer, where NK cell senescence coincides with iNKT hyperactivation in later cancer stages [27, 28]. These findings imply the potential involvement of NKT cells in the pathogenesis of both inflammation and tumor. NKT cells are functionally categorized into type I (also known as iNKT) and type II subsets based on α-GalCer reactivity. iNKT cells are reactive to α-GalCer and can bind to CD1d/α-GalCer tetramer, while type II NKT cells lack this responsiveness [29]. Moreover, these

subsets exhibit opposing immunomodulatory effects: iNKT cells demonstrate antitumor activity, whereas type II NKT cells often promote immunosuppression and tumor progression [30]. This functional ambiguity aligns with Torina's "time-dependent activation" hypothesis, where NKT cells initially secrete anti-inflammatory IL-10 but switch to pro-inflammatory IFN-γ upon prolonged stimulation [31]. It is possible that such temporal dynamics influence NKT subset differentiation. However, due to the limitations of the present study, we could not definitively assess the specific subset driving the NKT expansion and the pro- or anti-inflammatory role of NKT cells in MPP progression, underscoring the need for further in-depth research.

MDSCs are a diverse population of immature myeloid cells characterized by their potent immunosuppressive effects [32]. Importantly, the effects of PMN-MDSCs and M-MDSCs appear to depend on the infecting pathogens. PMN-MDSCs are predominantly observed in infections caused by Gram-positive bacteria, whereas M-MDSCs are commonly found in cases involving both Gram-positive and Gram-negative bacteria [33]. Considering that MP is a Gram-negative microorganism, it may have contributed to the higher levels of M-MDSCs and lower levels of PMN-MDSCs present in our MPP cases. Notably, there is also a bidirectional crosstalk between Treg and MDSCs, enhancing their synergistic immunosuppressive effects [32]. Thus, efforts to target cell surface molecules involved in MDSC-Treg interactions, such as PD1/PD-L1 and LAG-3/MHCII, could be a promising strategy to improve immunotherapeutic efficacy on MPP.

With the outbreak of MPP, researchers are increasingly focusing on efforts to identify clinical indicators of S-MPP. Although some of our findings align with previous studies (e.g., the correlation between disease severity and D-dimer or LDH) [34], our results differ in several respects. For instance, Zhang et al.. identified independent risk factors for S-MPP, including age, albumin-to-globulin ratio, CRP, etc [11]. Differences in region, age, and health conditions among MPP patients may contribute to these discrepancies. Finally, we evaluated various variables and proposed a unique predictive model utilizing IL-18, ChE, and naïve B cell percentage to differentiate S-MPP from NS-MPP cases. To our knowledge, this is the first time that ChE and naïve B cell percentage have been identified as markers of severe MPP, offering new perspectives on evaluating MPP cases.

Our study had some limitations. First, RMPP cases reportedly have a higher likelihood of progressing to severe disease compared with non-RMPP cases [35]. However, we were unable to identify immunological indicators to distinguish RMPP cases from non-RMPP cases because the prevailing MP strain is macrolide-resistant. Second, MPP cases and NMP cases we enrolled were actually in different disease stages. Hence, to yield a more reliable predictive model, the predictive factors for S-MPP were derived from the total MPP cases, excluding NMP cases. Third, this study did not focus on functional or mechanistic exploration of the immune signatures observed in children with MPP. We plan to pursue these types of exploration in future studies.

Conclusions

The MPP outbreak following the COVID-19 pandemic has underscored the need for a comprehensive understanding of this disease. In this study, we elucidated the clinical and immunological characteristics of MPP cases, particularly S-MPP, and developed a novel predictive model for S-MPP. These findings may facilitate clinical assessment of MPP cases and inspire innovative therapeutic strategies for children with MPP.

Abbreviations

ChE	Cholinesterase
HC	Healthy control
IFN	Interferon
IL-18	Interleukin 18
M-MDSC	Monocytic MDSC
MDSC	Myeloid-derived suppressor cells
Mono	Monocyte
MPP	Mycoplasma pneumoniae pneumonia
NKT	Natural killer T cell
NMP	Non-MPP pneumonia
NS-MPP	Non-severe MPP
PMN-MDSC	Polymorphonuclear MDSC
S-MPP	Severe MPP
Tfh	Follicular helper T cell
Tfr	Follicular regulatory T cell
Th1	T helper type 1
Treg	Regulatory T cell

Supplementary Information

The online version contains supplementary material available at https://doi.org/10.1186/s12931-025-03189-7.

Supplementary Material 1

Acknowledgements

Not applicable.

Author contributions

YZ, JX, XZ and YW conceived and designed the study. AL, YQ, DW, WH, QW, GL, LW and XZ collected patient specimens. RJ, CZ, ZC and YG conducted the experiments. RJ and HG analyzed the data. YZ, JX, RJ, and HG wrote the manuscript. All authors contributed to the article and approved the submitted version. All authors contributed to the article and approved the submitted version.

Funding

This work was supported by the National Key R&D Program of China (grant numbers 2024YFC3405903, 2021YFC2701800 and 2021YFC2701802) (to YZ); National Natural Science Foundation of China (grant numbers 82241038 and 81974248) (to YZ); Shanghai Committee of Science and Technology (grant numbers 21140902400, 23ZR1407600, and 21ZR1410000) (to YZ); Xiamen Key Healthcare Projects (grant numbers 3502Z20244005) (to YZ); "Medicine + X" Interdisciplinary Innovation Team Incubation Program (Key Project) of Children's Hospital of Fudan University (grant numbers EKYX202410) (to YZ);

Key Development Program of Children's Hospital of Fudan University (grant numbers EK2022ZX05) (to JX).

Data availability
The datasets analysed during the current study are available from the corresponding author on reasonable request.

Declarations

Ethics approval and consent to participate
The study was approved by the Ethics Committee of Children's Hospital of Fudan University [NO. 2023(249)]. The study was conducted in accordance with the local legislation and institutional requirements. Written informed consent for participation in this study was provided by the participants' legal guardians/next of kin.

Consent for publication
Not applicable.

Competing interests
The authors declare no competing interests.

Clinical trial number
Not applicable.

Author details
[1]Department of Clinical Laboratory, Children's Hospital of Fudan University, National Children's Medical Center, Shanghai, China
[2]Department of Critical Care Medicine, Children's Hospital of Fudan University, National Children's Medical Center, Shanghai, China
[3]The Shanghai Key Laboratory of Medical Epigenetics, International Co-laboratory of Medical Epigenetics and Metabolism, Ministry of Science and Technology, Institutes of Biomedical Sciences, Fudan University, Shanghai, China
[4]Key Laboratory of Neonatal Diseases, National Health Commission (NHC), Fudan University, Shanghai, China
[5]Department of Respiratory Medicine, Children's Hospital of Fudan University, Shanghai, China
[6]Department of Hematology/Oncology, Children's Hospital of Fudan University, Shanghai, China
[7]Shanghai Institute of Infectious Disease and Biosecurity, Fudan University, Shanghai, China
[8]Department of Neurology, Children's Hospital of Fudan University, Shanghai, China
[9]Fujian Key Laboratory of Neonatal Diseases, Xiamen Key Laboratory of Neonatal Diseases, Xiamen Children's Hospital (Children's Hospital of Fudan University at Xiamen), Xiamen, China

Received: 10 December 2024 / Accepted: 11 March 2025
Published online: 17 March 2025

References

1. Ding G, Zhang X, Vinturache A, van Rossum AMC, Yin Y, Zhang Y. Challenges in the treatment of pediatric Mycoplasma pneumoniae pneumonia. Eur J Pediatr. 2024;183(7):3001–11.
2. Meyer Sauteur PM, Beeton ML, Pereyre S, Bébéar C, Gardette M, Hénin N, et al. Mycoplasma pneumoniae: delayed re-emergence after COVID-19 pandemic restrictions. Lancet Microbe. 2024;5(2):e100–1.
3. Edouard S, Boughammoura H, Colson P, La Scola B, Fournier PE, Fenollar F. Large-scale outbreak of Mycoplasma pneumoniae infection, Marseille, France, 2023–2024. Emerging infectious diseases. 2024;30(7).
4. Meyer Sauteur PM, Beeton ML. Mycoplasma pneumoniae: delayed re-emergence after COVID-19 pandemic restrictions. Lancet Microbe. 2024;5(2):e100–1.
5. Kyi D, Xiao Y, Wang X, Feng S, Wang Y, Liao L et al. Predominance of A2063G mutant strains in the Mycoplasma pneumoniae epidemic in children-a clinical and epidemiological study in 2023 in Wuhan, China. Int J Infect Diseases: IJID: Official Publication Int Soc Infect Dis. 2024;145:107074.
6. Zhang XB, He W, Gui YH, Lu Q, Yin Y, Zhang JH, et al. Current Mycoplasma pneumoniae epidemic among children in Shanghai: unusual pneumonia caused by usual pathogen. World J Pediatrics: WJP. 2024;20(1):5–10.
7. Li H, Li S, Yang H, Chen Z, Zhou Z. Resurgence of Mycoplasma pneumonia by macrolide-resistant epidemic clones in China. Lancet Microbe. 2024;5(6):e515.
8. Gong H, Sun B, Chen Y, Chen H. The risk factors of children acquiring refractory Mycoplasma pneumoniae pneumonia: a meta-analysis. Medicine. 2021;100(11):e24894.
9. Lee K-L, Lee C-M, Yang T-L, Yen T-Y, Chang L-Y, Chen J-M, et al. Severe Mycoplasma pneumoniae pneumonia requiring intensive care in children, 2010–2019. J Formos Med Assoc. 2021;120(1, Part 1):281–91.
10. Shi S, Zhang X, Zhou Y, Tang H, Zhao D, Liu F. Immunosuppression reduces lung injury caused by Mycoplasma pneumoniae infection. Sci Rep. 2019;9(1):7147.
11. Zhang X, Sun R, Jia W, Li P, Song C. A new dynamic nomogram for predicting the risk of severe Mycoplasma pneumoniae pneumonia in children. Sci Rep. 2024;14(1):8260.
12. Pánisová E, Unger WWJ, Berger C, Meyer Sauteur PM. Mycoplasma pneumoniae-specific IFN-γ-producing CD4(+) effector-memory T cells correlate with pulmonary disease. Am J Respir Cell Mol Biol. 2021;64(1):143–6.
13. Dixon AE, Mandac JB, Martin PJ, Madtes DK, Hackman RC, Clark JG. Alloreactive Th1 cells localize in lung and induce acute lung injury. Chest. 1999;116(1 Suppl):s36–7.
14. Wang T, Sun H, Lu Z, Jiang W, Dai G, Huang L, et al. The CARDS toxin of Mycoplasma pneumoniae induces a positive feedback loop of type 1 immune response. Front Immunol. 2022;13:1054788.
15. Hoshino K, Tsutsui H, Kawai T, Takeda K, Nakanishi K, Takeda Y, et al. Cutting edge: generation of IL-18 receptor-deficient mice: evidence for IL-1 receptor-related protein as an essential IL-18 binding Receptor1. J Immunol. 1999;162(9):5041–4.
16. Novick D, Kim S, Kaplanski G, Dinarello CA. Interleukin-18, more than a Th1 cytokine. Semin Immunol. 2013;25(6):439–48.
17. Paul S, Chhatar S, Mishra A, Lal G. Natural killer T cell activation increases iNOS + CD206- M1 macrophage and controls the growth of solid tumor. J Immunother Cancer. 2019;7(1):208.
18. Sossou D, Ezinmegnon S, Agbota G, Gbedande K, Accrombessi M, Massougbodji A, et al. Regulatory T cell homing and activation is a signature of neonatal sepsis. Front Immunol. 2024;15:1420554.
19. Takahashi R, Shiohara T, Mizukawa Y. Monocyte-independent and -dependent regulation of regulatory T-cell development in Mycoplasma infection. J Infect Dis. 2021;223(10):1733–42.
20. Chu KA, Chen W, Hsu CY, Hung YM, Wei JC. Increased risk of rheumatoid arthritis among patients with Mycoplasma pneumonia: a nationwide population-based cohort study in Taiwan. PLoS ONE. 2019;14(1):e0210750.
21. Koch MA, Thomas KR, Perdue NR, Smigiel KS, Srivastava S, Campbell DJ. T-bet(+) Treg cells undergo abortive Th1 cell differentiation due to impaired expression of IL-12 receptor B2. Immunity. 2012;37(3):501–10.
22. Mijnheer G, Lutter L, Mokry M, van der Wal M, Scholman R, Fleskens V, et al. Conserved human effector Treg cell transcriptomic and epigenetic signature in arthritic joint inflammation. Nat Commun. 2021;12(1):2710.
23. Miyauchi K, Adachi Y, Tonouchi K, Yajima T, Harada Y, Fukuyama H, et al. Influenza virus infection expands the breadth of antibody responses through IL-4 signalling in B cells. Nat Commun. 2021;12(1):3789.
24. Rothaeusler K, Baumgarth N. B-cell fate decisions following influenza virus infection. Eur J Immunol. 2010;40(2):366–77.
25. Clement RL, Daccache J, Mohammed MT, Diallo A, Blazar BR, Kuchroo VK, et al. Follicular regulatory T cells control humoral and allergic immunity by restraining early B cell responses. Nat Immunol. 2019;20(10):1360–71.
26. Powell MD, Read KA, Sreekumar BK, Jones DM, Oestreich KJ. IL-12 signaling drives the differentiation and function of a TH1-derived TFH1-like cell population. Sci Rep. 2019;9(1):13991.
27. Liao CM, Zimmer MI, Wang CR. The functions of type I and type II natural killer T cells in inflammatory bowel diseases. Inflamm Bowel Dis. 2013;19(6):1330–8.
28. Liu X, Li L, Si F, Huang L, Zhao Y, Zhang C, et al. NK and NKT cells have distinct properties and functions in cancer. Oncogene. 2021;40(27):4521–37.
29. Duthoo E, Beyls E, Backers L, Gudjónsson T, Huang P, Jonckheere L et al. Replication stress, microcephalic primordial dwarfism, and compromised immunity in ATRIP deficient patients. J Exp Med. 2025;222(5).

30. Liao CM, Zimmer MI, Shanmuganad S, Yu HT, Cardell SL, Wang CR. Dysregulation of CD1d-restricted type Ii natural killer T cells leads to spontaneous development of colitis in mice. Gastroenterology. 2012;142(2):326–34.e1-2.
31. Torina A, Guggino G, La Manna MP, Sireci G. The Janus face of NKT cell function in autoimmunity and infectious diseases. Int J Mol Sci. 2018;19(2).
32. Haist M, Stege H, Grabbe S, Bros M. The functional crosstalk between myeloid-derived suppressor cells and regulatory T cells within the immunosuppressive tumor microenvironment. Cancers. 2021;13(2).
33. Gabrilovich DI, Editorial. The intricacy of choice: can bacteria decide what type of myeloid cells to stimulate? J Leukoc Biol. 2014;96(5):671–4.
34. Lee Y-C, Chang C-H, Lee W-J, Liu T-Y, Tsai C-M, Tsai T-A, et al. Altered chemokine profile in refractory Mycoplasma pneumoniae pneumonia infected children. J Microbiol Immunol Infect. 2021;54(4):673–9.
35. Bajantri B, Venkatram S, Diaz-Fuentes G. Mycoplasma pneumoniae: a potentially severe infection. J Clin Med Res. 2018;10(7):535–44.

Publisher's note